Riparian Ecohydrology: Regulation of Water Flux from the Ground to the Atmosphere in the Middle Rio Grande, New Mexico

James R. Cleverly[1*], Clifford N. Dahm[1], James R. Thibault[1] Dianne E. McDonnell[1,2], and Julie E. Allred Coonrod[2]

[1] Department of Biology, MSC03 2020, 1 University of New Mexico, Albuquerque, New Mexico, 87131-0001

[2] Department of Civil Engineering, MSC01 1070, 1 University of New Mexico, Albuquerque, New Mexico, 87131-0001

[*] Correspondence: cleverly@sevilleta.unm.edu, 505-277-9341, 505-277-6318 (FAX)

Abstract. During the previous decade, the southwestern United States has faced declining water resources and escalating forest fires due to long-term regional drought. Competing demands for water resources require a careful accounting of the basin water budget. Water lost to the atmosphere through riparian evapotranspiration (ET) is believed to rank in the top third of water budget depletions. To better manage depletions in a large river system, patterns of riparian ET must be better understood. This paper provides a general overview of the ecological, hydrological, and atmospheric issues surrounding riparian ET in the Middle Rio Grande of New Mexico. Long-term measurements of ET, water table depth, and micrometeorological conditions have been made at sites dominated by native cottonwood (*Populus deltoides*) forests and non-native saltcedar (*Tamarix chinensis*) thickets along the Middle Rio Grande (MRG). Over periods longer than one week, groundwater and leaf area index (LAI) dynamics relate well with ET rates. Evapotranspiration from *P. deltoides* forests was unaffected by annual drought conditions in much of the MRG where the water table is maintained above three meters below the surface. Evapotranspiration from a dense *T. chinensis* thicket did not decline with increasing groundwater depth; instead, ET increased by 50%, from 6 mm/day to 9 mm/day, as the water table receded at nearly 7 cm/day. Leaf area index of the *T. chinensis* thicket likewise increased during groundwater decline. Leaf area index can be manipulated as well following removal of non-native species. When *T. chinensis* and non-native Russian olive (*Elaeagnus angustifolia*) were removed from a *P. deltoides* understory, water salvaged through reduced ET was 26 cm/yr in relation to ET measured at reference sites. To investigate correlates to short-term variations in ET, stepwise multiple linear regression was used to evaluate atmospheric conditions under which ET is elevated or depressed. At the *P. deltoides*-dominated sites, ET anomalies were positively correlated to net radiation (R_n) and negatively correlated to sensible heat flux (H), cross-corridor wind speed (v), and along-corridor wind speed (u) ($r^2 = 0.54$). At the *T. chinensis*-dominated sites, ET anomalies were positively correlated with R_n, u, the friction coefficient (u_*), and vapor pressure deficit (VPD) and were negatively correlated to surface humidity scale (q_*), daily high and low temperature, H, and precipitation ($r^2 = 0.66$). Both *Tamarix* and *Populus* can transpire prodigious quantities of water when the conditions are as favorable. In the Middle Rio Grande, *T. chinensis* is preferentially found where summer flooding and cold air drainage occurs, and *P. deltoides* is preferentially located in locations with shallow groundwater within two meters of the surface.

Introduction

Riparian habitats worldwide are emerging as intense political, economic, social, and ecological battlegrounds over limited water resources (Zube and Simcox, 1987; Jackson *et al.*, 2001). In arid and semiarid regions, freshwater resources are concentrated along riparian corridors. These oases support high biodiversity, enhanced ecosystem productivity, and agricultural, municipal, and industrial demands for water (Malanson, 1995). The focus of human activities along rivers changes stream hydrology and ecology: perennial streams become ephemeral, diversions lower the water table, and plant stress leads to loss of native vegetation and shifts in species composition from native to non-native species (Medina, 1990; Smith *et al.*, 1991).

Increasing density of non-native species, along with declining ecological importance of native species, has been described in nearly all river systems throughout the western United States (Howe and Chancellor, 1983; Snyder and Miller, 1993; Di Tomaso, 1998; Pataki *et al.*, 2005; Shafroth *et al.*, 2005). The two most common non-native plants in western U.S. river corridors are *Tamarix* L. (saltcedar), and *Elaeagnus angustifolia* (Russian olive) (Friedman *et al.*, 2005). *Tamarix* spp. are primarily *T. ramosissima* and closely related *T. chinensis* and hereafter referred to as *Tamarix*. Both *Tamarix* and *E. angustifolia* originated in Eurasia, and they represent the third and fourth most common species found in western U.S. riparian areas, after *Salix exigua* (sandbar or coyote willow) and *Populus deltoides* (plains cottonwood) (Friedman *et al.*, 2005). The range of *E. angustifolia* is still expanding, while *Tamarix* dominance appears to be reaching an equilibrium in which expansion of *Tamarix* in some locations is balanced by loss of *Tamarix* in other locations (Friedman *et al.*, 2005). Examples of native species maintaining or

recovering community dominance have been observed in the Rio Grande and Colorado River systems (Snyder and Miller, 1993; Cleverly *et al.*, 1997; Nagler *et al.*, 2005b).

Riparian ecosystems that are prone to invasion by non-native species are characterized by greater disturbance frequency and intensity, deeper water tables, greater fluctuation of water table depth, greater surface salinity, and flood timing outside of the regeneration window for native species (Smith *et al.*, 1991; Busch and Smith, 1993; Busch and Smith, 1995; Planty-Tabacchi *et al.*, 1996; Lite and Stromberg, 2005; Tiegs *et al.*, 2005). Characteristics of *Tamarrix* that contribute to its ecological success include fruit production extending across the growing season; greater reproductive output; tolerance of heat, salinity, drought, and flooding stresses; regeneration following fire; induced sediment accretion with resultant deepening of the water table; surface soil salinization; and profligate transpiration from both groundwater and soil water sources (Warren and Turner, 1975; Busch *et al.*, 1992; Sala *et al.*, 1996; Di Tomaso, 1998; Cleverly *et al.*, 2002). Extensive reviews of *Tamarix* and *E. angustifolia* invasion ecology have been provided by Di Tomaso (1998) and Katz and Shafroth (2003), respectively.

The potential for non-native vegetation to remove prolific quantities of water from the ground is of serious concern to water resource managers, although a great deal of controversy continues to exist regarding water use by *Tamarix* (Hughes, 1993; Shafroth *et al.*, 2005). This controversy is driven by estimates of *Tamarix* water use that vary wildly, depending upon habitat and upon how water use is measured or estimated (Hughes, 1993; Cleverly *et al.*, 2002; Shafroth *et al.*, 2005). This paper will present a case study in riparian evapotranspiration along the Middle Rio Grande (MRG), New Mexico, U.S.A. There were two main objectives of this study: (1) to determine the relative evapotranspirational water losses from non-native and native riparian species under a range of natural environmental variations (Cleverly *et al.*, 2002; Dahm

et al., 2002); and (2) to investigate short- and long-term patterns of variability in measured ET for evaluating potential water salvage of riparian restoration and vegetation management (Molles *et al.*, 1998; Shafroth *et al.*, 2005; Newman *et al.*, In Review).

Evapotranspiration

Evapotranspiration (ET) is the process by which water is transported from the surface to the atmosphere as water vapor. Evapotranspiration is the combined evaporation from soil, open water, and ice surfaces, along with transpiration from vegetation. In riparian areas, the presence of shallow groundwater provides an ample water supply, permitting greater annual ET rates than precipitation (PPT) (Dahm *et al.*, 2002; Huxman *et al.*, 2005). Because ET from most ecosystems within a large basin is limited by PPT, riparian corridors exist as a hot spot of water loss to the atmosphere within large arid- and semiarid basins (Devitt *et al.*, 1998; Kurc and Small, 2004; Huxman *et al.*, 2005). Soil evaporation is negligible under riparian canopies due to attenuation of radiation by vegetation (Saugier and Katerji, 1991; Wilson *et al.*, 2001). Riparian ecosystems are characterized by a high transpiration to evapotranspiration ratio in the southwestern United States (Kurc and Small, 2004; Huxman *et al.*, 2005; Newman *et al.*, In Review).

Water budgeting has long been used to integrate large-scale surface water and groundwater dynamics. In large river systems, uncertainty in estimating the numerous pathways through which water can enter or leave a basin requires the use of the best "guesses" for depletions such as riparian ET, groundwater–recharge, and surface water–groundwater interactions (Scott *et al.*, 2000; Cleverly *et al.*, 2002; Dahm *et al.*, 2002). Of these depletions, ET from phreatophytes such as *P. deltoides* and *S. exigua* represents most of the 20 to 50 percent of total long-term

water budget depletions that are ascribed to natural vegetation (Scott *et al.*, 2000; Dahm *et al.*, 2002).

Many methods used for estimating ET are based upon the application of the energy balance, or conservation of incoming and outgoing energy. Under steady state conditions, and assuming a closed system, energy entering the canopy will be balanced by energy leaving the canopy:

$$R_n = \lambda E + H + G\,, \tag{1}$$

where R_n is the net radiation, λE is latent heat flux, H is sensible heat flux, and G is the ground heat flux (W m^{-2}). Net radiation is the difference between downward- and upward-directed radiative energy flux:

$$R_n = (Q_{L\downarrow} + Q_{S\downarrow}) - (Q_{L\uparrow} + Q_{S\uparrow})\,, \tag{2}$$

where Q is radiative energy flux, L and S represent long-wave (i.e., thermal) and shortwave (i.e., solar) radiation, respectively. The direction of the arrow indicates whether radiation is directed down into the canopy or up away from the canopy. By convention, R_n is positive when directed toward the surface, and the remaining terms are positive when directed away from the surface. Latent heat flux represents the energy absorbed or released when water changes phase. Ground heat flux is the heat conducted through the soil surface, and H is the convective energy flux generated by atmospheric temperature gradients.

The Bowen ratio energy balance (BREB) method, for example, has been used for decades to estimate *Tamarix* ET (Gay and Fritschen, 1979; Devitt *et al.*, 1998). This method utilizes measurements of R_n, G, and the Bowen ratio, β, to determine λE:

$$\beta = \frac{H}{\lambda E} = \frac{C_P}{\lambda \varepsilon} \frac{(T_2 - T_1)}{(\chi_2 - \chi_1)}\,, \tag{3}$$

where C_p is the heat capacity of air, λ is the latent heat of vaporization, T is temperature, ε is the ratio of the molecular weights of water and dry air, and χ is the mole fraction of the partial pressure of water vapor. Temperature and humidity are each measured at heights two heights above the canopy where the subscript 2 refers to the upper measurement. Latent heat flux is determined as the residual of the energy balance (Eq. 1):

$$\lambda E = \frac{R_n - G}{1 + \beta}. \quad (4)$$

Bowen ratio energy balance methods have been applied successfully in wetlands with adequate fetch and a homogeneous canopy (Drexler *et al.*, 2004). Even when these conditions are met, however, energy balance estimates of ET can be confounded by sensible heat advection, which is the horizontal movement of momentum, energy, or other scalar quantities across a heterogeneous landscape (Itier *et al.*, 1994; McAneney *et al.*, 1994; Devitt *et al.*, 1998; Cooper *et al.*, 2000; Drexler *et al.*, 2004). Advection occurs when wet surfaces, such as wetlands or irrigated ecosystems, are located adjacent to dry surfaces such as arid and semi-arid rangeland ecosystems. Sensible heat advection into riparian forests is most easily identified when the evaporative fraction, which is the ratio $\lambda E:R_n$, is greater than unity (Devitt *et al.* 1998).

Three-dimensional sonic eddy covariance (3SEC) is the benchmark method for measuring fluxes over tall vegetation, under advection, and in complex terrain is (Brunet *et al.*, 1994; McAneney *et al.*, 1994; Simpson *et al.*, 1998; Drexler *et al.*, 2004). One advantage of the 3SEC system is that ET is measured directly, rather than estimated as the residual of the energy balance (Eq. 4). Thus, 3SEC is the only method that provides the means of estimating energy balance closure error as a self-check for accuracy (Twine *et al.*, 2000; Drexler *et al.*, 2004).

The core instruments in 3SEC systems are a 3-D sonic anemometer to measure wind speed in three dimensions, a krypton hygrometer or an infrared gas analyzer (IRGA) to measure humidity, a thermocouple with a very fine-wire junction (0.0127 mm diameter type E chromel–constantan) to avoid signal retention in high frequency measurements, and an IRGA to measure CO_2 concentration. Each of these instruments make measurements at a frequency determined through spectral decomposition of sample time series taken at 20 Hz. A sampling frequency is chosen in the high-frequency spectral gap, usually between 5 and 20 Hz (Stull, 1988).

Latent heat flux (λE), or the heat absorbed by evaporation, is computed from these measurements as a function of the covariance between vertical wind speed and humidity:

$$\lambda E = \lambda \overline{w'q'} = \lambda \sum_{i=1}^{n} \frac{(w_i - \bar{w})(q_i - \bar{q})}{n} = \lambda \mathrm{Cov}(wq) = \lambda \rho_w \mathrm{ET}, \quad (5)$$

where λ is the latent heat of vaporization, w' is the instantaneous deviation from mean vertical wind speed (i.e., $w' = w_i - \bar{w}$), and q' is the instantaneous deviation from average water vapor density. The time period for averaging, n, is chosen from balancing the spectral gap with minimizing trending in very low frequencies. Covariance periods are typically 15 to 40 minutes long. Sensible heat flux (H, heat transfer due to vertical atmospheric temperature gradients) is computed likewise as a function of the covariance between vertical wind speed and temperature:

$$H = C_p \rho_a \overline{w'T'} = C_p \rho_a \sum_{i=1}^{n} \frac{(w_i - \bar{w})(T_i - \bar{T})}{n} = C_p \rho_a \mathrm{Cov}(wT), \quad (6)$$

where ρ_a is density of wet air, and T' is the instantaneous deviation of temperature from mean air temperature.

Before ET is computed from LE, various standard corrections are applied to incorporate the physical realities within which these measurements are made. These corrections include coordinate rotation to align the wind vector with the sonic anemometer (Wesely, 1970),

corrections developed from frequency response relationships which incorporate sensor line averaging and separation (Massman, 2000; Massman, 2001), correction to account for flux effects on vapor density measurements as opposed to mixing ratio measurements (Webb *et al.*, 1980), and krypton hygrometer oxygen and second-order humidity effects on vapor density measurements. Lastly, closure of the energy balance is forced into thermodynamic equilibrium by adding closure energy into H and λE in relation to the measured Bowen ratio (Twine *et al.*, 2000; Cleverly *et al.*, 2002).

Measurement of turbulent fluxes via 3SEC involves measuring flux variables from a tower or an aircraft. When measurements made from a tower, the minimum spacing between a canopy and the sensors is dictated by the necessity to make measurements above the roughness sublayer. The top of the roughness sublayer is equal to the distance of the aerodynamic roughness length, z_0, above the canopy, h_c (Nakamura and Mahrt, 2001). The upper limit for sensor placement in riparian corridors is chosen to remain below the top of the surface layer and to minimize the measurement footprint (Cooper *et al.*, 2000; Cooper *et al.*, 2003b). The top of the surface layer is defined in terms of Monin-Obukhov theory, which describes the physics of the atmospheric surface layer (Stull, 1988). Atmospheric stability imposed by advection is associated with vertical thermal stratification and compression of the surface layer to the lower few meters above the canopy (Cooper *et al.*, 2003b).

The planetary boundary layer is that lower portion of the atmosphere where turbulence dominates vertical transport and friction creates a strong drag on near-surface winds. The surface layer makes up the bottom 10% of the boundary layer (Stull, 1988), were surface drag creates a near-logarithmic wind speed profile. The vertical gradient in horizontal wind speed causes deformation of the air column and generates turbulence that can be characterized by

Reynolds stress, $\tau_{Reynolds}$, which is equal to the total vertical flux of horizontal momentum in the surface layer (Stull, 1988):

$$\left|\tau_{\text{Reynolds}}\right| = \bar{\rho}\left[\left(\overline{u'w'}\right)^2 + \left(\overline{v'w'}\right)^2\right]^{1/2} \tag{7}$$

where ρ is density of air, and u, v, and w are orthogonal wind speeds in two horizontal and one vertical dimensions, respectively. The velocity scale across which Reynolds stresses are propagated is the friction coefficient, u_* (Stull, 1988):

$$u_* = \frac{\left|\tau_{\text{Reynolds}}\right|}{\rho} = \left[\left(\overline{u'w'}\right)^2 + \left(\overline{v'w'}\right)^2\right]^{1/2} \tag{8}$$

The friction coefficient is important in describing the magnitude of turbulence in the surface layer, and that prominence is central to the body of the relationships known as Monin-Obukhov (M-O) similarity theory. M-O similarity theory, also known as surface layer similarity theory, is a body of empirical relationships that characterize turbulence in the surface layer. Other M-O scales useful for characterizing the surface layer include the humidity scale, q_*^{SL}, the temperature scale, θ_*^{SL}, and the Obukhov length, L (Stull, 1988):

$$q_* = \frac{-\overline{w'q'}}{u_*}, \tag{9}$$

$$\theta_* = \frac{-\overline{w'T'}}{u_*}. \tag{10}$$

$$L = \frac{-\bar{T}u_*^2}{kg\theta_*} \tag{11}$$

where k is von Kármán's constant and g is the acceleration due gravity. When L is zero, the surface layer is neutrally stratified. When negative, the surface layer is unstably stratified, and the temperature profile in the surface layer is stable when L is positive.

The measurement footprint represents the upwind distance that is incorporated into measurements made by instruments on the tower. The footprint increases with height above the canopy and with wind speed (Rannik *et al.*, 2000). In riparian forests along the Middle Rio Grande and the San Pedro River, the footprint for sensors mounted 2.5-m above *Tamarix* may be as little as 40 to 60 m under ideal conditions, or up to 200 m over *Populus fremontii* (Fremont cottonwood) and *Sporobolus wrightii* (sacaton grass) (Cooper *et al.*, 2000; Cooper *et al.*, 2003b).

The Middle Rio Grande

The Middle Rio Grande is located in New Mexico, U.S.A. and is defined to coincide with the New Mexico delivery obligation supply index gauges near Otowi NM and at Elephant Butte Dam, set forth in the Rio Grande compact (revised 1948). The MRG has three tributaries within the basin: the Jemez River, the Rio Puerco, and the Rio Salado (Fig. 1). The Rio Puerco and Rio Salado contribute flood flow to the MRG during summer monsoon periods. Three dams divert water from the Rio Grande to support irrigated agriculture (Fig. 1): the angostura diversion dam downstream of the confluence between the Rio Grande and the Jemez River, the Isleta pueblo diversion dam downstream of Albuquerque NM, and the San Acacia diversion dam downstream of the confluence of the Rio Grande with the Rio Salado. Three more dams create reservoirs in the MRG basin (Fig. 1): at Cochiti Pueblo, at Jemez Pueblo, and at Elephant Butte near Truth or Consequences NM. Elephant Butte Lake is the only reservoir with significant storage capacity, and the remaining reservoirs are principally operated for flood control. Mountainous terrain, identified in a 100-m resolution digital elevation model, was identified in the northern and southern portions of the MRG, while the Albuquerque and Belen reaches are overlooked by mesas (Fig. 1).

Flood control was promoted by the addition of riverside drains and levees during the early to mid 20th century. Exceptionally high flows in the river are contained within undeveloped riparian zones through the construction of levees. Adjacent to this levee system are drains that were excavated to an elevation below river channel bottom. These drains were placed to generate a hydrologic gradient away from the valley bottom, thus curtailing flooding beyond the levees. Excess water applied in irrigation is leached into the drain system.

One further significant hydrologic feature is the City of Albuquerque's wastewater reclamation plant. This plant was originally established in 1962 and contributes ca. 40% of the tributary inflow to the MRG, not including trans-basin transfers and tributary inflow in the upper Rio Grande basin above Otowi (Cleverly *et al.*, 2002; Dahm *et al.*, 2002). The origin of this water is pumped from the deep paleoaquifer at stations throughout the Albuquerque sub basin, providing long-term water resources to the MRG.

In arid and semi-arid regions, water loss to the atmosphere in riparian corridors dominate basin water budgets, representing well over 90% of Middle Rio Grande (MRG) depletions due to open water evaporation, soil evaporation, transpiration, and irrigated agriculture (Cleverly *et al.*, 2002; Dahm *et al.*, 2002). Evapotranspiration from riparian vegetation has been estimated to represent 30% of the total depletions in the MRG water budget.

Since the early twentieth century, riparian vegetation density and cover has been slowly increasing in all reaches of the Upper and Middle Rio Grande due to anthropogenic modifications of the MRG's hydrology (Everitt, 1998). On the Rio Grande upstream of its confluence with the Rio Puerco, *P. deltoides* cover has been increasing (Snyder and Miller, 1993). By the 1960's, woody vegetation cover reached a maximum in the MRG at Albuquerque, where *P. deltoides* represented nearly all of the 75% ground cover (Campbell and Dick-Peddie,

1964). Downstream of the Rio Grande's confluence with the Rio Puerco, *Tamarix* thickets and woodlands have expanded the area covered by woody vegetation while *P. deltoides* cover has decreased (Howe and Knopf, 1991; Everitt, 1998) (Fig. 1).

Currently, dense monocultures of non-native *Tamarix chinensis* Lour. (saltcedar) dominate the floodplain downstream of the Rio Grande's confluence with the Rio Puerco (Fig. 1). These thickets cover 100% of the land surface between riverside levees. In contrast, reaches of the Rio Grande upstream of the Rio Puerco's confluence are fully covered by a dense *Populus deltoides* ssp. *wislizeni* (S. Watson) Eckenw. (Rio Grande cottonwood) forests. In many locations, these *P. deltoides* forests include a dense understory of non-native species, predominately *Elaeagnus angustifolia* L. (Russian olive) and *Tamarix* (Fig. 1).

Study area and methods

Four sites were chosen in 1998. Two locations of large extent were identified in *P. deltoides* forests, one with a short (i.e., less than three years) interflood interval, and the other with a long (i.e., greater than 40 years) interflood interval. Two *Tamarix* stands were likewise chosen with short and long interflood intervals (Molles *et al.*, 1998). The northernmost site, located in the south valley of Albuquerque, New Mexico, hosted a sparse *P. deltoides* forest (122 trees ha^{-1}) and a very dense understory thicket of *Tamarix* and *E. angustifolia* until 2004, when the understory was removed as part of a citywide restoration project (Fig. 1). The other *P. deltoides*-dominated site, located near the towns of Belen and Rio Communities NM, regularly receives flooding and supports a high-density forest (278 trees ha^{-1}) with predominantly native understory species. In November 1999, a 25-m tower was established to measure ET in each of these *P. deltoides* forests.

The northernmost *Tamarix*-dominated site is located at the Sevilleta National Wildlife Refuge (NWR), home of the Sevilleta Long Term Ecological Research (LTER) program. This site is located between the confluence of the Rio Salado and the San Acacia diversion structure, and the vegetation is a mosaic of *Tamarix* thickets, *D. spicata* meadows, and various halophytes like *Prosopis pubescens* Benth. (screwbean mesquite) and *Atriplex* L. spp (saltbush). A 10-m eddy covariance tower was established at this site in March 1999. The second *Tamarix*-dominated site is located at Bosque del Apache NWR. This site is frequently flooded and contains a dense (15,000 shrubs ha^{-1}), monospecific *Tamarix* thicket. The U.S. Bureau of Reclamation and New Mexico State University established a 15-m tower in this thicket in 1998.

Three-dimensional eddy covariance system were mounted on the towers, 2 to 2.5 meters above the canopy (Cleverly *et al.*, 2002; Dahm *et al.*, 2002). The measurement period was 10 Hz and the covariance period was 30 minutes. Additional energy flux measurements were made at 1 Hz and averaged over 30 minutes. Net radiation was measured using annually cross-calibrated REBS Q7.1 net radiometers. Ground heat flux was measured using Campbell Scientific, Inc. (CSI) ground heat flux plates, corrected for heat storage in the 8 cm of soil above the plate using soil temperature (CSI TCAV) and soil water content (CSI CS616) measurements. Average energy balance closure for all systems in all years, determined on a daily basis, was 78%, and the Bowen ratio was near zero during the growing season (Cleverly *et al.*, 2002). These are values typical of eddy covariance and riparian corridors, respectively (Devitt *et al.*, 1998; Wilson *et al.*, 2002).

Complementary measurements made from each tower include standard weather station conditions (i.e., precipitation, temperature, relative humidity, horizontal wind speed and direction; Campbell Scientific, Inc., Logan, UT). Measurements of vapor pressure were used to

calculate vapor pressure deficit (VPD) as the difference between atmospheric vapor pressure (e_a, kPa) and saturation vapor pressure (e_s, kPa). This difference represents the vapor pressure gradient from the saturated tissues within a leaf to the free atmosphere.

A network of five shallow groundwater wells was placed at each site, with one well near the tower and four additional wells in the four cardinal directions, 40-m from the central well. Three of the wells at each of the sites were equipped with automated pressure transducers, measuring water level every 30 minutes (EEI, Las Cruces, NM). In 2003, all five wells at each site were instrumented with pressure transducers, with a subset of those also measuring groundwater temperature (Solinst Canada Ltd, Georgetown, Ontario).

Plant area index (PAI), which is the projected area of leaves and stems per unit ground area, was measured from below relatively undisturbed vegetation adjacent to each of five groundwater wells using the LAI2000 (Li-cor, Inc., Lincoln, NE). Two measurements above the canopy and five measurements below the canopy were made in each plot. The first and second plots were double-sampled to track changes in measured PAI with changing light conditions. Measurements were made monthly during the growing season, as well as once during the winter of 2001-2002 to estimate stem area index (SAI). Retention by *P. deltoides* of senescent leaves through the winter confounds the winter measurement from *P. deltoides* forests. Measurements were made either during 45 minutes between sundown and dark or, weather permitting, under cloud cover. Measurements of clear sky conditions were made from a ladder or from the tower at *Tamarix* sites and from the nearby levee at *P. deltoides* sites because the vegetation is taller than 20-m.

Plant area index is equal to the sum of the projected LAI and SAI, less the area of overlap between stems and leaves. In broadleaf species such as *P. deltoides*, overlap between stem area

and leaf area is the same as SAI, thus PAI equals projected LAI. (Gower and Norman, 1991; Chen and Black, 1992; Chen and Cihlar, 1995; Chen and Cihlar, 1996). Incorporation of leaf geometry was considered in three leaf types: broadleaf tree (i.e., *P. deltoides* and *E. angustifolia*), flat leaf shrubs (i.e., *Salix exigua*), and cylindrically-leaved shrubs (i.e., *Tamarix*). Leaf area index of the three-dimensional leaf surface was determined for each leaf type as:

$$LAI(broadleaf)_{total} = 2 \bullet PAI \tag{12}$$

$$LAI(flat)_{total} = 2 \bullet (PAI - SAI) \tag{13}$$

$$LAI(cylindrical)_{total} = \pi \bullet (PAI - SAI) \tag{14}$$

Stepwise multiple linear regression (proc GLM, Statistical Analysis Software, SAS Institute, Inc., Cary, NC) was used to evaluate effect of micrometeorological conditions on daily ET rates (Nagler *et al.*, 2005a). A suite of micrometeorological variables was chosen for the analysis representing surface layer aerodynamics, energy fluxes, and standard weather phenomena (Table 2). Because temporal autocorrelation in micrometeorological time series data violate the critical regression assumption of independent and identically distributed (i.i.d.) measurements, anomaly analysis was chosen to resample the time series and thereby eliminate i.i.d. restrictions (Higgins *et al.*, 1997). Evapotranspiration anomalies are identified as having a value greater or lesser than one standard deviation from average, computed as the 9-day running average, $\overline{ET_{9-day}}$. These n=43±3 anomalies per year from each tower are then used as the dependent variable in both forward and reverse steps. This analysis indicates which micrometeorological conditions are related to driving daily ET above or below the long-term average.

Drought and Groundwater (slow dynamics)

In the year 2000, the *P. deltoides* forest with a non-native understory had the highest annual ET (Albuquerque) (Table 1). The lowest ET in every year was generated by the xeroriparian *Tamarix* woodland at the Sevilleta NWR (Table 1). This xeroriparian *Tamarix* woodland was also distinguished by having the highest ET:LAI ratio of all the sites (Table 1). The vegetation in this location is predominantly a mosaic of *Tamarix* and *D. spicata*. *Prosopis pubescens* (screwbean mesquite) and *Atriplex* spp. are also present at the Sevilleta site. Of the sites with intermediate annual ET, monospecific *Tamarix* (Bosque del Apache NWR) lost more water through ET than the *P. deltoides* forest containing a mostly native understory (Belen—Rio Communities) (Table 1). Average annual precipitation is 20 to 31 cm in the MRG (Dahm *et al.*, 2002), and the ET:PPT ratio was greater than unity at all sites in all years.

Removal of non-native species from the understory of a *P. deltoides* forest had a modest effect on forest ET. Evapotranspiration decreased by 9% following removal of non-native species between 2003 and 2004 (Table 1). However, ET at both of the *Tamarix*-dominated sites increased in 2004 by 12% over 2003 ET (Table 1). Assuming that the *Tamarix* sites are representing the reference conditions for ET water loss in the basin, the net decrease in ET due to removal of non-native species is 21%, a savings of 26 cm in the first year following clearing. While this value is consistent with earlier predictions, water salvage may be short-lived because *Tamarix* and *E. angustifolia* were allowed to regenerate during the 2005 growing season (data not shown) (Shafroth *et al.*, 2005). Greater reduction in ET is expected to follow from converting a monospecific saltcedar stand (e.g., Bosque del Apache NWR) into a saltgrass or meadow (Shafroth *et al.*, 2005).

Recurrent, extended drought in the southwestern United States, also referred to as "megadrought," is characterized decreased regional precipitation in both the winter and summer modes. Recently, research has shown long-term sea surface temperature anomalies to be related to these megadroughts, in which the Pacific decadal oscillation is in a cool phase (PDO-) and the Atlantic multi-decadal is in a warm phase (AMO+) (Gray *et al.*, 2003). Resultant decline of regional precipitation and snowpack is initially ameliorated in the riparian corridor by release from reservoir storage, maintaining surface flow and groundwater resources. Along the MRG, droughts have recurred every 20 to 70 years (Gray *et al.*, 2003).

Drought is expected to have an important recurring effect upon the MRG water budget, especially in naturally occurring processes like ET from riparian vegetation. Reduction in ET from *P. deltoides* stands was minimal, even during extreme drought (Table 1). The vegetation did not experience the full intensity of what has been considered a major drought because municipal wastewater maintained the water table within two meters of the surface at the Albuquerque site (Table 1 and Fig. 2). Likewise, groundwater dynamics follow a hydrograph of irrigation operations rather than a natural flow regime at the Belen site (data not shown). Flow in the riverside drain maintained the water table above 175 cm below the surface (Table 1). As long as the irrigation and wastewater treatment systems are in operation, ET depletions from *P. deltoides* forests remain undimished (Table 1).

Evapotranspiration and LAI declined in the *Tamarix* sites during drought (Table 1). Evapotranspiration at the Sevilleta NWR's *Tamarix* and *D. spicata* woodland tracked drought severity index values closely (Table 1). Bosque del Apache NWR's monospecific *Tamarix* thicket initially followed this trend, but ET and LAI began returning to pre–drought levels one year early, in 2003 (Table 1). Groundwater levels also declined with drought at the *Tamarix*

sites, especially during the late summer (Table 1 and Fig. 2). Groundwater levels and annual variability had not begun to return to pre-drought patterns in 2004, the first year following relief from meteorological drought (Table 1 and Fig. 2).

Evapotranspiration is often modeled as a function of groundwater depth (McDonald and Harbaugh, 1988). In the earliest conceptualization of this relationship, an elevation was defined above which ET is not limited by groundwater availability (i.e., $ET_{surface}$). At some deeper elevation, ET drops to zero because the water table is too deep for roots to access (i.e., $ET_{extinction}$). Surface and extinction elevations are species specific. In *P. deltoides*, for example, these depths are $ET_{surface}$ = 3-m and $ET_{extinction}$ = 5-m (Horton *et al.*, 2001). In fact, *P. deltoides* is well known for intolerance to groundwater recession, and crown dieback has been observed when the water table falls below three meters (Scott *et al.*, 1999; Rood *et al.*, 2000; Cooper *et al.*, 2003a). *P. deltoides*-dominated forests are typically found in places with a shallow and stable water table (Table 1 and Fig. 2).

While $ET_{surface}$ and $ET_{extinction}$ are well defined in *P. deltoides*, depth to groundwater has not been found to restrict *Tamarix* ET, even when the water table is 10 m (Horton *et al.*, 2001) or 25 m (Gries *et al.*, 2003) below the surface. In the latter study, water storage in sand dunes sustained transpiration because *Tamarix* is a facultative phreatophyte capable of exploiting soil water in addition to groundwater (Busch *et al.*, 1992; Smith *et al.*, 1998). *Tamarix* tend to occupy sites with groundwater depth variability (Lite and Stromberg, 2005), and that is true at Bosque del Apache NWR where water table fluctuates more than 350 cm per year (Fig. 2).

Water table depth was deepest in *Tamarix*-dominated sites (Table 1). In 2003, the water table at Bosque del Apache NWR fell below 3.5 meters for the first time in this study (Fig. 2). Groundwater decline was extreme that summer, falling as rapidly as seven cm day^{-1} (Fig. 3) from

175 cm below surface in May to 360 cm in September (Fig. 2). While crown dieback occurred in a nearby *P. deltoides* forest (data not shown), a resurgence in *Tamarix* ET accompanied groundwater recession (Table 1 and Fig. 3). ET from this *Tamarix* thicket increased substantially within a few days following the initiation of groundwater decline. Recently, Naumburg et al (2005) proposed a mechanism that explains this counterintuitive finding.

For species like *Tamarix* that are not susceptible to moderate soil drying (Pockman and Sperry, 2000), a receding water table can increase the volume of aerated soil near field capacity (Naumburg *et al.*, 2005). Draining of the soil is slower than the potential root growth rates in *Tamarix*, and the partly drained soil can be easily exploited (Naumburg *et al.*, 2005). The initial delay results from the time required for the capillary fringe of the original water table (GW_0 = 175 cm) to drain sufficiently to allow respiration and root growth below GW_0. Once this hypothetical taproot growth is initiated, water uptake by new root growth at depths greater than GW_0 is augmented by continued fine root functioning at GW_0. Fine roots at the previous capillary fringe continue to function because *Tamarix*, unlike *P. deltoides*, is relatively tolerant of low xylem water potential (Pockman and Sperry, 2000).

A few days before 1 July, ET decreased and groundwater recession slowed (Fig. 3). Stand ET declined again at the end of the year, preceding the year's maximum water table depth (GW_{max}) (Figs. 2 & 3). Decreased groundwater decline rate and ET near the beginning of July was caused by multi-day monsoon precipitation, during which net radiation and vapor pressure deficit (VPD) were minimized (data not shown). When that system had passed, groundwater decline and enhanced ET returned (Fig. 3).

Dependence upon the shallow aquifer may be related to phreatophytic status (Smith *et al.*, 1998). Thicket forming *Tamarix* spp. in the western U.S. are facultative phreatophyte using

water of an isotopic ratio intermediate between groundwater and precipitation sources (Busch *et al.*, 1992). In *Populus* spp., use of precipitation water sources is conditional upon access to groundwater; in locations with a deep water table or ephemeral access to a shallow water table, *Populus* spp. utilize both deep and shallow water sources (Stromberg and Patten, 1996; Snyder and Williams, 2000). Of the dominant species along the MRG, *Elaeagnus angustifolia* (Russian olive) is extremely varied in the habitats in which it thrives, but little has been documented regarding distributions where the groundwater is more than a few meters below the surface (Katz and Shafroth, 2003).

Average high and low temperature varied only slightly during between 2000 and 2004 (Table 1). The southern sites experience hotter days and colder nights than the northern sites (Table 1). This unusual pattern of minimum temperatures decreasing downstream can be explained by considering the distinct topographic features surrounding each site (Papadopoulos and Helmis, 1999). Katabatic winds, better known as cold air drainage, tends to be greatest in gullies and in mountainous terrain (Papadopoulos and Helmis, 1999; Soler *et al.*, 2001). These mountainous hillsides have slopes that increase in angle from the valley floor to mountain peaks. Because sunrise does not illuminate the entire east-facing slope at once, an inversion layer is formed just below the sunrise line. Katabatic flow continues below this inversion layer and anabatic flow begins above (Papadopoulos and Helmis, 1999). Because of the mountainous terrain near the downstream reaches of the MRG, cold air drainage into the *Tamarix* thickets maintains colder nighttime temperature (Table 1).

Flooding and Micro-meteorology (rapid dynamics)

Limited flooding of two sites, Belen—Rio Communities and Bosque del Apache NWR, occurred during spring 2001 due to a one-day release of 115 $m^3 s^{-1}$ from Cochiti Reservoir by the

US Army Corps of Engineers (Fig. 4). The travel time of this flood pulse was 48 hours between these two sites (Fig. 4). At Bosque del Apache, floodwater flowed into the floodplain over the bank 0.5 to 1 km upstream of the tower. Surface flow traveled parallel to the river, in contrast to flooding near Rio Communities, where stagnant open water arose from seepage. Surface inundation was short-lived at both sites, and the water table peaked for a single day (Fig. 4).

During onsite flooding, groundwater levels in the monitoring wells failed to reach the surface at either flooded site. At the northern cottonwood-dominated site, the water table reached the surface in some locations but not others, averaging 55 cm below the average land (Fig. 4). Local topographical relief is 50 cm between the highest and lowest-lying wells, but these wells represent only a fraction of the total topographic relief. Surface flooding was likewise observed in depressions but not ridges within the active floodplain.

Total ET from this *P. deltoides* forest did not increase during or following inundation (Fig. 4). Net radiation reaching the forest floor through the canopy is minimal, generally between 50 and 100 W m^{-2}, providing little energy for forest floor evaporation (Wilson *et al.*, 2001). At the same time, transpiration is not curtailed completely due to root hypoxia, for only a fraction of the active roots are likely to be under the water table.

Flooding in the monospecific *Tamarix* thicket was associated with elevated total ET rates (Fig. 4). Unlike the loamy sand underlying the *P. deltoides* forest, the soil at this site is dominated by loamy clay. The Rio Puerco is well known for generating a load of very fine sediments into the MRG (Phippen and Wohl, 2003; Gellis *et al.*, 2004). Fine sediments defloculate when wetted, creating an infiltration barrier. Therefore, the top meter of soil did not reach field capacity even though surface water was observed around all groundwater wells (Fig. 4).

Evapotranspiration rates were closely coupled to VPD at the *Tamarix* sites (Table 3 and Fig. 4). *Tamarix*' cylindrical leaves form a minimal boundary layer, and stomata respond rapidly to atmospheric conditions and thereby closely link transpiration to micro-meteorological conditions (Table 3) (Jarvis and McNaughton, 1986; Hollinger *et al.*, 1994; Meinzer *et al.*, 1997; Nagler *et al.*, 2005a). At the *P. deltoides* sites, coupling between VPD and ET was observed for a part of the year, but asynchrony between VPD and ET fluctuations was observed during flooding (Fig. 4). On average, short-term fluctuations in *P. deltoides* ET were not closely coupled to fluctuations in VPD (Table 3).

Coupling between ET and atmospheric conditions was closer at the *Tamarix* sites than at the *P. deltoides* sites (Table 3 and Fig. 5). Evapotranspiration from the *Tamarix* canopy was especially sensitive to aerodynamic characteristics of the surface layer (Table 3). Variations in u_* are observed under advection, when temperature inversions within the lower atmosphere constrain the extent of the surface layer (Cooper *et al.*, 2003b).

Precipitation decreases ET and H at the *Tamarix* sites through shading and the resulting reduction in R_n (Table 3). Because vegetation along the MRG are not water limited due to the close proximity of groundwater (Table 1 and Fig. 2), precipitation does not directly lead to changes in ET (Table 3), in contrast to the flush of leaf gas exchange that follows precipitation in drier riparian habitats (Huxman *et al.*, 2004). The interaction of daily temperature extremes also contributed to the micro-meteorological control of *Tamarix* ET (Tables 1 & 3) (Nagler *et al.*, 2005a).

Energy balance and horizontal wind direction explained slightly more than 50% of the daily variability in *P. deltoides* ET (Table 3 and Fig. 5). Sensible heat advection, carried on the wind tangential to the riparian corridor, and the development of a thick local boundary layer,

reduces the coupling between stomatal conductance, vapor pressure deficit, and transpiration (Table 3) (Jarvis and McNaughton, 1986). Sensible heat advection and surface layer dynamics had a stronger effect on *P. deltoides* ET in Albuquerque's south valley than in Belen (data not shown).

Modeled ET anomalies fit well with measured anomalies, especially at the *Tamarix* sites (Fig. 5). Residuals from the regression analysis were evenly distributed around the model line (Fig. 5), suggesting that the anomaly dataset is essentially free from autocorrelation bias (Nagler *et al.*, 2005a). For the most part, energy balance and aerodynamics are related to short-term fluctuations in riparian ET (Table 3) (Pieri and Fuchs, 1990). Variables that were included in the analysis, but which did not show any relationship to ET fluctuations, included depth to groundwater, G, and barometric pressure (Tables 2 & 3). Ground heat flux is near zero and does not vary (data not shown). Depth to groundwater does vary, but at a slower scale that could not be detected in the short-term analysis.

Conclusions

Evapotranspiration rates were compared among native and non-native riparian vegetation along the Middle Rio Grande in New Mexico. Evapotranspiration from xeroriparian shrubs, including non-native *Tamarix* and native *D. spicata,* was lower than ET from any other vegetation class (Table 1). Highest ET rates were measured from a multi-layered canopy site in which non-native *Tamarix* and *E. angustifolia* formed a thick understory with a *P. deltoides* forest (Table 1). However, the monospecific *Tamarix* and native *P. deltoides* forest without a dense non-native understory also support ET rates greater than 100 cm yr^{-1}, which is three to five times annual precipitation in the basin (Table 1) (Dahm *et al.*, 2002). Energy balance closure

error was 78%, well within the 10%-30% range for eddy covariance systems (Twine *et al.*, 2000).

Reduction in ET following removal of the non-native understory from a *P. deltoides* canopy resulted in a modest 21% reduction in ET relative to the reference sites (Table 1) (Shafroth *et al.*, 2005). However, ET at the post-removal was lower than it had been in any other year at that site, it was the first year this site did not support higher ET rates than any other site. Water salvage will be transitory, however, should the understory be allowed to regenerate its non-native understory. To be economically feasible, an emphasis upon long-term success in restoration projects needs to be pursued.

Evapotranspiration rates responds to groundwater depth, stomatal coupling to atmospheric humidity, leaf area index, atmospheric surface layer conditions, and energy balance. The recent severe drought had little effect on native *P. deltoides* forests because water tables were artificially maintained to within two meters of the surface, but *Tamarix* water use and LAI were diminished under drought conditions (Table 1). However, water table decline during drought resulted in 50% higher ET rates from a dense, monospecific *Tamarix* thicket (Fig. 3). Evapotranspiration from *Tamarix* is closely coupled to atmospheric conditions rather than water table depth (Table 3 and Fig. 4). Evapotranspiration from *P. deltoides* is responsive to variations in energy balance and sensible heat advection rather than atmospheric humidity or temperature (Table 3) (Horton *et al.*, 2001).

Acknowledgments

The authors would like to thank Laurence Hipps, John Prueger, Daniel Cooper, and Salim Bawazir for their conceptual, computational, and methodological assistance. We would like to further thank the Society of Range Management for sponsoring the symposium that lead to the

preparation of this paper. Site access was granted by the Sevilleta NWR, Bosque del Apache NWR, La Joya State Game Refuge, the Middle Rio Grande Conservancy District, New Mexico's state forestry department, and the city of Albuquerque's open space division. Further thanks for their ongoing interest are offered to the Hydrogeoecology and the Sevilleta Long Term Ecological Research groups at the University of New Mexico, the New Mexico interagency ET workgroup, the Bosque Hydrology Group, and the New Mexico State EPSCoR office. This research has been funded by NASA award NAG5-6999, the New Mexico Interstate Stream Commission, the U.S. Fish and Wildlife Service's Bosque Initiative, the U.S. Bureau of Reclamation's Endangered Species Workgroup, and a NSF-EPSCoR Research Infrastructure award. We would finally like to thank three anonymous reviewers for their assistance in improving an early version of this manuscript.

References

Brunet Y, Itier B, McAneney J, and Lagouarde JP. 1994. Downwind evolution of scalar fluxes and surface resistance under conditions of local advection. Part II: Measurements over barley. *Agricultural and Forest Meteorology* **71**: 227-245.

Busch DE, Ingraham NL, and Smith SD. 1992. Water uptake in woody riparian phreatophytes of the Southwestern United States: a stable isotope study. *Ecological Applications* **2**: 450-459.

Busch DE, and Smith SD. 1993. Effects of fire on water and salinity relations of riparian woody taxa. *Oecologia* **94**: 186-194.

Busch DE, and Smith SD. 1995. Mechanisms associated with decline of woody species in riparian ecosystems of the southwestern U.S. *Ecological Monographs* **65**: 347-370.

Campbell CJ, and Dick-Peddie WA. 1964. Comparison of phreatophytic communities on the Rio Grande in New Mexico. *Ecology* **45**: 492-502.

Chen JM, and Black TA. 1992. Defining leaf-area index for non-flat leaves. *Plant Cell and Environment* **15**: 421-429.

Chen JM, and Cihlar J. 1995. Quantifying the effect of canopy architecture on optical measurements of leaf-area index using 2 gap size analysis-methods. *IEEE Transactions On Geoscience and Remote Sensing* **33**: 777-787.

Chen JM, and Cihlar J. 1996. Retrieving leaf area index of boreal conifer forests using landsat TM images. *Remote Sensing of Environment* **55**: 153-162.

Cleverly JR, Dahm CN, Thibault JR, Gilroy DJ, and Coonrod JEA. 2002. Seasonal estimates of actual evapo-transpiration from *Tamarix ramosissima* stands using three-dimensional eddy covariance. *Journal of Arid Environments* **52**: 181-197.

Cleverly JR, Smith SD, Sala A, and Devitt DA. 1997. Invasive capacity of *Tamarix ramosissima* in a Mojave Desert floodplain: the role of drought. *Oecologia* **111**: 12-18.

Cooper D, D'Amico D, and Scott M. 2003a. Physiological and morphological response patterns of *Populus deltoides* to alluvial groundwater pumping, *Environmental Management*, **31**: 215-226. doi: 10.1007/s00267-002-2808-2.

Cooper D, Eichinger W, Archuleta J, Hipps L, Kao J, Leclerc M, Neale C, and Prueger J. 2003b. Spatial source-area analysis of three-dimensional moisture fields from LIDAR, eddy covariance, and a footprint model. *Agricultural and Forest Meteorology* **114**: 213-234.

Cooper DI, Eichinger WE, Holtkamp DB, Karl RR, Jr., Quick CR, Dugas W, and Hipps L. 1992. Spatial variability of water vapor turbulent transfer within the boundary layer. *Boundary-Layer Meteorology* **61**: 389-405.

Cooper DI, Eichinger WE, Kao J, Hipps L, Reisner J, Smith S, Schaeffer SM, and Williams DG. 2000. Spatial and temporal properties of water vapor and latent energy flux over a riparian canopy. *Agricultural and Forest Meteorology* **105**: 161-183.

Dahm CN, Cleverly JR, Coonrod JEA, Thibault JR, McDonnell DE, and Gilroy DF. 2002. Evapotranspiration at the land/water interface in a semi-arid drainage basin. *Freshwater Biology* **47**: 831-843.

Devitt DA, Sala A, Smith SD, Cleverly J, Shaulis LK, and Hammett R. 1998. Bowen ratio estimates of evapotranspiration for *Tamarix ramosissima* stands on the Virgin River in southern Nevada. *Water Resources Research* **34**: 2407-2414.

Di Tomaso J. 1998. Impact, biology, and ecology of saltcedar (Tamarix spp.) in the southwestern United States. *WEED TECHNOLOGY* **12**: 326-336.

Drexler JZ, Snyder RL, Spano D, and Paw U KT. 2004. A review of models and micrometeorological methods used to estimate wetland evapotranspiration, *Hydrological Processes*. doi: 10.1002/hyp.1462.

Everitt B. 1998. Chronology of the spread of tamarisk in the central Rio Grande. *Wetlands* **18**: 658-668.

Friedman JM, Auble GT, Shafroth PB, Scott ML, Merigliano MF, Preehling MD, and Griffin EK. 2005. Dominance of non-native riparian trees in western USA. *Biological Invasions* **7**: 747-751.

Gay LW, and Fritschen LJ. 1979. An energy budget analysis of water use by saltcedar. *Water Resources Research* **15**: 1589-1592.

Gellis AC, Pavich MJ, Bierman PR, Clapp EM, Ellevein A, and Aby S. 2004. Modern sediment yield compared to geologic rates of sediment production in a semi-arid basin, New Mexico: Assessing the human impact. *Earth Surface Processes And Landforms* **29**: 1359-1372.

Gower ST, and Norman JM. 1991. Rapid estimation of leaf-area index in conifer and broad-leaf plantations. *Ecology* **72**: 1896-1900.

Gray S, Betancourt J, Fastie C, and Jackson S. 2003. Patterns and sources of multidecadal oscillations in drought-sensitive tree-ring records from the central and southern Rocky Mountains. *Geophysical Research Letters* **30**: 1316.

Gries D, Zeng F, Foetzki A, Arndt S, Bruelheide H, Thomas F, Zhang X, and Runge M. 2003. Growth and water relations of *Tamarix ramosissima* and *Populus euphratica* on

Taklamakan desert dunes in relation to depth to a permanent water table. *Plant, Cell and Environment* **26**: 725-736.
Higgins RW, Yao Y, and Wang XL. 1997. Influence of the North American monsoon system on the US summer precipitation regime. *Journal of Climate* **10**: 2600-2622.
Hollinger DY, Kelliher FM, Schulze E-D, and Köstner BMM. 1994. Coupling of tree transpiration to atmospheric turbulence. *Nature* **371**: 60-62.
Horton JL, Kolb TE, and Hart SC. 2001. Physiological response to groundwater depth varies among species and with river flow regulation. *Ecological Applications* **11**: 1046-1059.
Howe CD, and Chancellor RJ. 1983. Factors affecting the viable seed content of soils beneath lowland pastures. *Journal of Applied Ecology* **20**: 915-922.
Howe WH, and Knopf FL. 1991. On the imminent decline of Rio Grande cottonwoods in central New Mexico. *Southwestern Naturalist* **36**: 218-224.
Hughes LE. 1993. "The devil's own"--Tamarisk. *Rangelands* **15**: 151-155.
Huxman TE, Snyder KA, Tissue D, Leffler AJ, Ogle K, Pockman WT, Sandquist DR, Potts DL, and Schwinning S. 2004. Precipitation pulses and carbon fluxes in semiarid and arid ecosystems. *Oecologia* **141**: 254-268.
Huxman TE, Wilcox BP, Breshears DD, Scott RL, Snyder KA, Small EE, Hultine K, Pockman WT, and Jackson RB. 2005. Ecohydrological implications of woody plant encroachment. *Ecology* **86**: 308-319.
Itier B, Brunet Y, McAneney KJ, and Lagouarde JP. 1994. Downwind evolution of scalar fluxes and surface resistance under conditions of local advection. Part I: A reappraisal of boundary conditions. *Agricultural and Forest Meteorology* **71**: 211-225.
Jackson RB, Carpenter SR, Dahm CN, McKnight DM, Naiman RJ, Postel SL, and Running SW. 2001. Water in a changing world. *Ecological Applications* **11**: 1027-1045.
Jarvis PG, and McNaughton KG. 1986. Stomatal control of transpiration: scaling up from leaf to region. *Advances in Ecological Research* **15**: 1-49.
Katz G, and Shafroth P. 2003. Biology, ecology and management of *Elaeagnus angustifolia* L. (Russian olive) in western North America. *Wetlands* **23**: 763-777.
Kurc SA, and Small EE. 2004. Dynamics of evapotranspiration in semiarid grassland and shrubland ecosystems during the summer monsoon season, central New Mexico. *Water Resources Research* **40**: W09305.
Lite SJ, and Stromberg JC. 2005. Surface water and ground-water thresholds for maintaining Populus-Salix forests, San Pedro River, Arizona. *Biological Conservation* **125**: 153-167.
Malanson GP. 1995. *Riparian Landscapes*. Cambridge University Press, Cambridge, UK.
Massman W. 2000. A simple method for estimating frequency response corrections for eddy covariance systems. *Agricultural and Forest Meteorology* **104**: 185-198.
Massman W. 2001. Reply to comment by Rannik on "A simple method for estimating frequency response corrections for eddy covariance systems". *Agricultural and Forest Meteorology* **107**: 247-251.
McAneney KJ, Brunet Y, and Itier B. 1994. Downwind evolution of transpiration by two irrigated crops under conditions of local advection. *Journal of Hydrology* **161**: 375-388.
McDonald MG, and Harbaugh AW. 1988. A modular three-dimensional finite-difference ground-wtaer flow model. US Geological Survey. TWI 6-A1
Medina AL. 1990. Possible effects of residential development on streamflow, riparian plant communities, and fisheries on small mountain streams in central Arizona. *Forest Ecology and Management* **33**: 1-4.

Meinzer FC, Hinckley TM, and Ceulemans R. 1997. Apparent responses of stomata to transpiration and humidity in a hybrid poplar canopy. *Plant Cell and Environment* **20**: 1301-1308.

Molles MC, Crawford CS, Ellis LM, Valett HM, and Dahm CN. 1998. Managed flooding for riparian ecosystem restoration : Managed flooding reorganizes riparian forest ecosystems along the middle Rio Grande in New Mexico. *Bioscience* **48**: 749-756.

Nagler PL, Cleverly J, Glenn E, Lampkin D, Huete A, and Wan ZM. 2005a. Predicting riparian evapotranspiration from MODIS vegetation indices and meteorological data. *Remote Sensing of Environment* **15**: 17-30.

Nagler PL, Hinojosa-Huerta O, Glenn EP, Garcia-Hernandez J, Romo R, Curtis C, Huete AR, and Nelson SG. 2005b. Regeneration of native trees in the presence of invasive saltcedar in the Colorado River delta, Mexico. *Conservation Biology* **19**: 1842-1852.

Nakamura R, and Mahrt L. 2001. Similarity theory for local and spatially averaged momentum fluxes. *Agricultural and Forest Meteorology* **108**: 265-279.

Naumburg E, Mata-Gonzalez R, Hunter RG, Mclendon T, and Martin DW. 2005. Phreatophytic vegetation and groundwater fluctuations: A review of current research and application of ecosystem response modeling with an emphasis on Great Basin vegetation. *Environmental Management* **35**: 726-740.

Newman BD, Wilcox BP, Archer S, Breshears DD, Dahm CN, Duffy CJ, McDowell NG, Phillips FM, Scanlon BR, and Vivoni ER. In Review. The ecohydrology of arid and semiarid environments: a scientific vision. *Water Resources Research*.

Papadopoulos K, and Helmis C. 1999. Evening and morning transition of katabatic flows. *Boundary-Layer Meteorology* **92**: 195-227.

Pataki DE, Bush SE, Gardner P, Solomon DK, and Ehleringer JR. 2005. Ecohydrology in a Colorado River riparian forest: Implications for the decline of Populus fremontii. *Ecological Applications* **15**: 1009-1018.

Phippen SJ, and Wohl E. 2003. An assessment of land use and other factors affecting sediment loads in the Rio Puerco watershed, New Mexico. *Geomorphology* **16**: 3-4.

Pieri P, and Fuchs M. 1990. Comparison of Bowen Ration and aerodynamic estimates of evapotranspiration. *Agricultural and Forest Meteorology* **49**: 243-256.

Planty-Tabacchi A-M, Tabacchi E, Naiman RJ, Deferrari C, and Decamps H. 1996. Invasibility of species-rich communities in riparian zones. *Conservation Biology* **10**: 598-607.

Pockman W, and Sperry J. 2000. Vulnerability to xylem cavitation and the distribution of Sonoran desert vegetation. *American Journal of Botany* **87**: 1287-1299.

Rannik U, Aubinet M, Kurbanmuradov O, Sabelfeld K, Markkanen T, and Vesala T. 2000. Footprint analysis for measurements over a heterogeneous forest. *Boundary-Layer Meteorology* **97**: 137-166.

Rood S, Patino S, Coombs K, and Tyree M. 2000. Branch sacrifice: cavitation-associated drought adaptation of riparian cottonwoods. *Trees: Structure and Function* **14**: 248-257.

Sala A, Devitt DA, and Smith SD. 1996. Water use by *Tamarix ramosissima* and associated phreatophytes in a Mojave Desert floodplain. *Ecological Applications* **6**: 888-898.

Saugier B, and Katerji N. 1991. Some plant factors controlling evapotranspiration. *Agricultural and Forest Meteorology* **54**: 263-277.

Scott ML, Shafroth PB, and Auble GT. 1999. Responses of riparian cottonwoods to alluvial water table declines. *Environmental Management* **23**: 347-358.

Scott RL, Shuttleworth WJ, Goodrich DC, and Maddock T. 2000. The water use of two dominant vegetation communities in a semiarid riparian ecosystem. *Agricultural and Forest Meteorology* **105**: 241-256.

Shafroth PB, Cleverly JR, Dudley TL, Taylor JP, Van Riper C, Weeks EP, and Stuart JN. 2005. Control of *Tamarix* in the Western United States: Implications for water salvage, wildlife use, and riparian restoration. *Environmental Management* **35**: 231-246.

Simpson IJ, Thurtell GW, Neumann HH, Den Hartog G, and Edwards GC. 1998. The validity of similarity theory in the roughness sublayer above forests. *Boundary-Layer Meteorology* **87**: 69-99.

Smith SD, Devitt DA, Sala A, Cleverly JR, and Busch DE. 1998. Water relations of riparian plants from warm desert regions. *Wetlands* **18**: 687-696.

Smith SD, Wellington AB, Nachlinger JL, and Fox CA. 1991. Functional responses of riparian vegetation to streamflow diversion in the eastern Sierra Nevada. *Ecological Applications* **1**: 89-97.

Snyder K, and Williams D. 2000. Water sources used by riparian trees varies among stream types on the San Pedro River, Arizona. *Agricultural and Forest Meteorology* **105**: 227-240.

Snyder WD, and Miller GC. 1993. Changes in riparian vegetation along the Colorado River and Rio Grande, Colorado. *Great Basin Naturalist* **52**: 357-363.

Soler M, Infante C, Buenestado P, and Mahrt L. 2001. Observations of nocturnal drainage flow in a shallow gully. *Boundary-Layer Meteorology* **105**: 253-273.

Stromberg J, and Patten D. 1996. Instream flow and cottonwood growth in the eastern Sierra Nevada of California, USA. *Regualate Rivers-Research & Management* **12**: 1-12.

Stull RB. 1988. *An Introduction to Boundary Layer Meteorology*. Kluwer Academic Publishers, Boston, MA.

Tiegs SD, O'Leary JF, Pohl MM, and Munill CL. 2005. Flood disturbance and riparian species diversity on the Colorado River Delta. *Biodiversity and Conservation* **14**: 1175-1194.

Twine TE, Kustas WP, Norman JM, Cook DR, Houser PR, Meyers TP, Prueger JH, Starks PJ, and Wesely ML. 2000. Correcting eddy-covariance flux underestimates over a grassland. *Agricultural and Forest Meteorology* **103**: 279-300.

Warren DK, and Turner RM. 1975. Saltcedar (Tamarix chinesis) seed production, seedling establishment, and response to inundation. *Journal of the Arizona Academy of Sciences* **10**: 135-144.

Webb E, Pearman G, and Leuning R. 1980. Correction of flux measurements for density effects due to heat and water-vapor transfer. *Quarterly Journal of the Royal Meteorological Society* **106**: 85-100.

Wesely ML. 1970. Eddy Correlation Measurements in the Atmospheric Surface Layer over Agricultural Crops, Ph.D. Dissertation, 102 pp., University of Wisconsin, Madison.

Wilson K, Baldocchi D, Aubinet M, Berbigier P, Bernhofer C, Dolman H, Falge E, Field C, Goldstein A, Granier A, Grelle A, Halldor T, Hollinger D, Katul G, Law B, Lindroth A, Meyers T, Moncrieff J, Monson R, Oechel W, Tenhunen J, Valentini R, Verma S, Vesala T, and Wofsy S. 2002. Energy partitioning between latent and sensible heat flux during the warm season at FLUXNET sites, *Water Resources Research*, **38**: 1294. doi: 10.1029/2001WR000989.

Wilson K, Hanson P, Mulholland P, Baldocchi D, and Wullschleger S. 2001. A comparison of methods for determining forest evapotranspiration and its components: sap-flow, soil

water budget, eddy covariance and catchment water balance. *Agricultural and Forest Meteorology* **106**: 153-168.

Zube EH, and Simcox DE. 1987. Arid lands, riparian landscapes, and management conflicts. *Environmental Management* **11**: 529-535.

Table 1. Summary of drought severity, annual evapotranspiration (ET, cm yr^{-1}), temperature extremes, and groundwater depth. Average annual Palmer drought severity index (PDSI) scores are the average monthly values from New Mexico regions 2 (North-central New Mexico) and 5 (Middle Rio Grande) (http://www.ncdc.noaa.gov/oa/climate/onlineprod/drought/xmgrg3.html). More negative PDSI values indicate increasingly severe drought. Average daily temperature extremes, both nightly low (T_{min}) and the daytime high (T_{max}), were calculated as an average of the same 92 days in each year: 14 – 23 May, 13 – 16 June, 21 June – 2 July, 11 – 12 July, 10 – 15 August, and 1 September – 28 October. Maximum daily average groundwater depth (GW_{max}) was measured from a well within five meters of each tower.

	Year:	2000	2001	2002	2003	2004
Site	PDSI:	-0.04	1.01	-3.39	-3.94	-0.09
	ET (cm/yr):	134	125	127	125	114
Albuquerque	T_{min} / T_{max}	12.3 / 26.5	12.0 / 27.1	12.1 / 26.5	12.9 / 27.4	12.1 / 26.0
*Populus deltoides**	LAI_{Total}	6.6 ± 0.2	7.0 ± 0.2	6.4 ± 0.2	4.0 ± 0.2	--
	Gw_{max} (cm)	(171)	(175)	(178)	(190)	(186)
	ET (cm/yr):	103	107	95	126	--
Belen	T_{min} / T_{max}	12.4 / 27.2	11.2 / 27.9	11.7 / 27.5	12.2 / 28.9	--
Populus deltoides	LAI_{Total}	5.0 ± 0.2	6.4 ± 0.2	6.0 ± 0.2	5.2 ± 0.2	--
	Gw_{max} (cm)	(118)	(139)	(155)	(168)	(163)
	ET (cm/yr):	86	83	71	69	80
Sevilleta NWR	T_{min} / T_{max}	10.1 / 28.6	8.8 / 29.5	9.2 / 28.5	9.8 / 29.6	8.6 / 27.8
*Tamarix chinensis***	LAI_{Total}	3.5 ± 0.1	1.6 ± 0.2	0.9 ± 0.1	1.6 ± 0.2	--
	Gw_{max} (cm)	(213)	(218)	(227)	(245)	(240)
	ET (cm/yr):	118	115	87	101	114
Bosque del Apache NWR	T_{min} / T_{max}	9.7 / 28.6	7.8 / 29.2	9.2 / 29.4	9.3 / 30.4	9.0 / 28.1
Tamarix chinensis	LAI_{Total}	4.7 ± 0.1	5.0 ± 0.1	2.5 ± 0.1	4.1 ± 0.1	--
	Gw_{max} (cm)	(267)	(288)	(347)	(385)	(376)

* dense non-native understory removed winter 2003/2004

** mosaic with *Distchlis spicata*, *Prosopis pubescens*, and *Atriplex* spp.

Table 2. Variables evaluated in stepwise multiple regression. During each iteration, variables with a probability of a type II error > 0.1 ($p > 0.1$) was removed from the analysis.

Variable	Units	Definition
Energy Balance:		
R_n	W m^{-2}	Daytime Net Radiation
H	W m^{-2}	Sensible Heat Flux
G	W m^{-2}	Ground Heat Flux
Aerodynamics:		
u	m s^{-1}	Daytime Windspeed along riparian corridor
v	m s^{-1}	Daytime Windspeed across (i.e., tangential to) riparian corridor
ws	m s^{-1}	Daytime 2-D Horizontal windspeed
nu	m s^{-1}	Nighttime windspeed along riparian corridor
nv	m s^{-1}	Nighttime windspeed across riparian corridor
nws	m s^{-1}	Nighttime 2-D Horizontal windspeed
u_*	m s^{-1}	Friction coefficient or velocity
q_*	g_{water} g_{air}^{-1}	Humidity scale in the surface layer
L	m	Obukhov Length
Meteorological Conditions:		
GDD	°C	Growing Degree Days
PPT	mm day^{-1}	Precipitation
q	g_{water} g_{air}^{-1}	Specific Humidity
T_{max}	°C	Daily High Temperature
T_{min}	°C	Daily Low Temperature
T	°C	Daily Average Temperature
VPD	kPa	Vapor pressure deficit
P	kPa	Atmospheric Pressure
Other:		
GW	cm	Depth to groundwater

Table 3. Results of stepwise multiple regression model between evapotranspiration anomalies and micrometeorological conditions. ET anomalies were identified when daily ET was more than one standard deviation above or below the 9-day running average. For ease of interpretation, factors related to ET anomalies are separated into energy, aerodynamic, and meteorological conditions. See text and Table 2 for descriptions of the modeled dependent variables. Models for predicting ET anomalies are [$ET_{anomaly}$ = – 0.008 H + 0.02 R_n – 0.1 v – 0.09 (v X u)] (r^2 = 0.54) in cottonwood forests and [$ET_{anomaly}$= 0.005 R_n + 0.08 u + 1.2 u_* – 4.2 q_* + 11.8 (u_* X q_*) – 0.5 VPD – 0.01 (T_{max} X T_{min}) – 0.003 (PPT X H) + 0.001 (R_n X PPT)] (r^2 = 0.66) for saltcedar stands.

Factor	Coefficient ± se	F	p
Albuquerque and Belen — Rio Communities, *Populus deltoides*			
Model:	**0.54**	**110.8**	**< 0.0001**
Energy Balance:			
H	-0.008 ± 0.002	19.2	< 0.0001
R_n	0.02 ± 0.0008	388.1	< 0.0001
Aerodynamics:			
v	-0.1 ± 0.06	5.8	0.02
v X u	-0.09 ± 0.02	16.2	< 0.0001
Sevilleta and Bosque del Apache NWRs, *Tamarix chinensis*			
Model:	**0.66**	**77.7**	**< 0.0001**
Energy Balance:			
R_n	0.005 ± 0.0005	83.7	< 0.0001
Aerodynamics:			
u	0.08 ± 0.03	7.5	0.007
u_*	1.2 ± 0.3	12.9	0.0004
q_*	-4.2 ± 0.6	50.2	< 0.0001
u_* X q_*	11.8 ± 4.3	7.4	0.007
Meteorological Conditions:			
VPD	0.5 ± 0.07	43.0	< 0.0001
T_{max} X T_{min}	-0.01 ± 0.003	9.8	0.002
Interacting Effects:			
PPT X H	-0.003 ± 0.0005	24.3	< 0.0001
R_n X PPT	0.001 ± 0.0003	18.4	< 0.0001

Figure Legends

Figure 1. Map of the Middle Rio Grande in New Mexico, USA. Locations of local cities are marked in the inset map. The Middle Rio Grande, originating in Otowi NM and discharging from Elephant Butte Reservoir, is dominated in the north by *Populus deltoides* ssp. *wislizeni* (Rio Grande cottonwood) and by *Tamarix chinensis* (saltcedar) in the southern reaches. Locations of nearby mountain ranges are illustrated, along with diversion dams, reservoirs, and tributaries. Four sites with tower-based eddy covariance systems are listed along with site locations and local riparian vegetation.

Figure 2. Daily average depth to groundwater (cm) in Albuquerque's South Valley (ABQ) and at Bosque del Apache NWR (BDA). Pressure transducer measurements were logged once every 30-min from within five meters of the tower.

Figure 3. Temporal pattern of mean changes in groundwater depth and mean *Tamarix chinensis* evapotranspiration (ET) in 2003 at Bosque del Apache National Wildlife Refuge. Change in groundwater depth is the difference between mean water table depth between two consecutive days, $dGW/dt = GW_{t-1} - GW_t$ where t is a discrete day. Negative values indicate a falling water table. Groundwater depth change and ET were smoothed with a 9-day running average. Refer to Figure 2 for daily depth to water table. The first day of each month is highlighted, and arrows follow the progression of the growing season.

Figure 4. Time series of daily evapotranspiration (ET), vapor pressure deficit (VPD), and depth to groundwater. Floodwaters were present at the Belen — Rio Communities *Populus deltoides* ssp. *wislizeni* (A) and Bosque del Apache *Tamarix chinensis* (B) sites on May 24 and May 26, 2001, respectively. The arrows in panel A and the first pair of arrows in panel B point

to the day of inundation. The two following pairs of arrows in panel B point to days of following ET maxima.

Figure 5. Measured and predicted evapotranspiration anomalies. Predicted anomalies were defined as the solution to the best-fit stepwise multiple linear regression model (Table 3).

Figure 1:

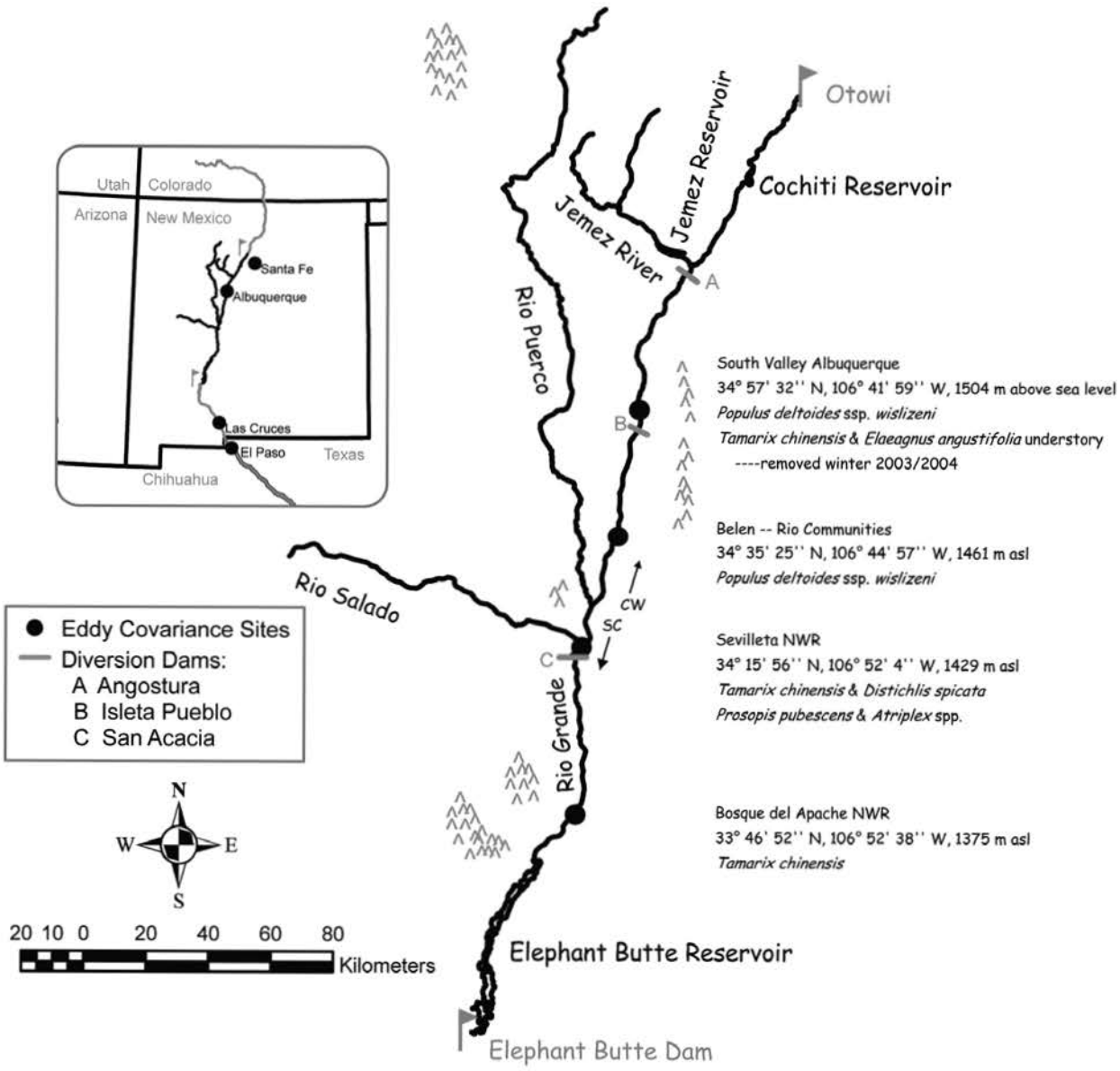
Utah
Colorado
Arizona
New Mexico
Santa Fe
Albuquerque
Las Cruces
El Paso
Texas
Chihuahua
Eddy Covariance Sites
Diversion Dams:
A Angostura
B Isleta Pueblo
C San Acacia
N
W
E
S
20 10 0 20 40 60 80
Kilometers
Otowi
Cochiti Reservoir
Jemez Reservoir
Jemez River
Rio Puerco
Rio Salado
Rio Grande
A
B
C
CW
SC
South Valley Albuquerque
34° 57' 32'' N, 106° 41' 59'' W, 1504 m above sea level
Populus deltoides ssp. wislizeni
Tamarix chinensis & Elaeagnus angustifolia understory
----removed winter 2003/2004
Belen -- Rio Communities
34° 35' 25'' N, 106° 44' 57'' W, 1461 m asl
Populus deltoides ssp. wislizeni
Sevilleta NWR
34° 15' 56'' N, 106° 52' 4'' W, 1429 m asl
Tamarix chinensis & Distichlis spicata
Prosopis pubescens & Atriplex spp.
Bosque del Apache NWR
33° 46' 52'' N, 106° 52' 38'' W, 1375 m asl
Tamarix chinensis
Elephant Butte Reservoir
Elephant Butte Dam

Figure 2:

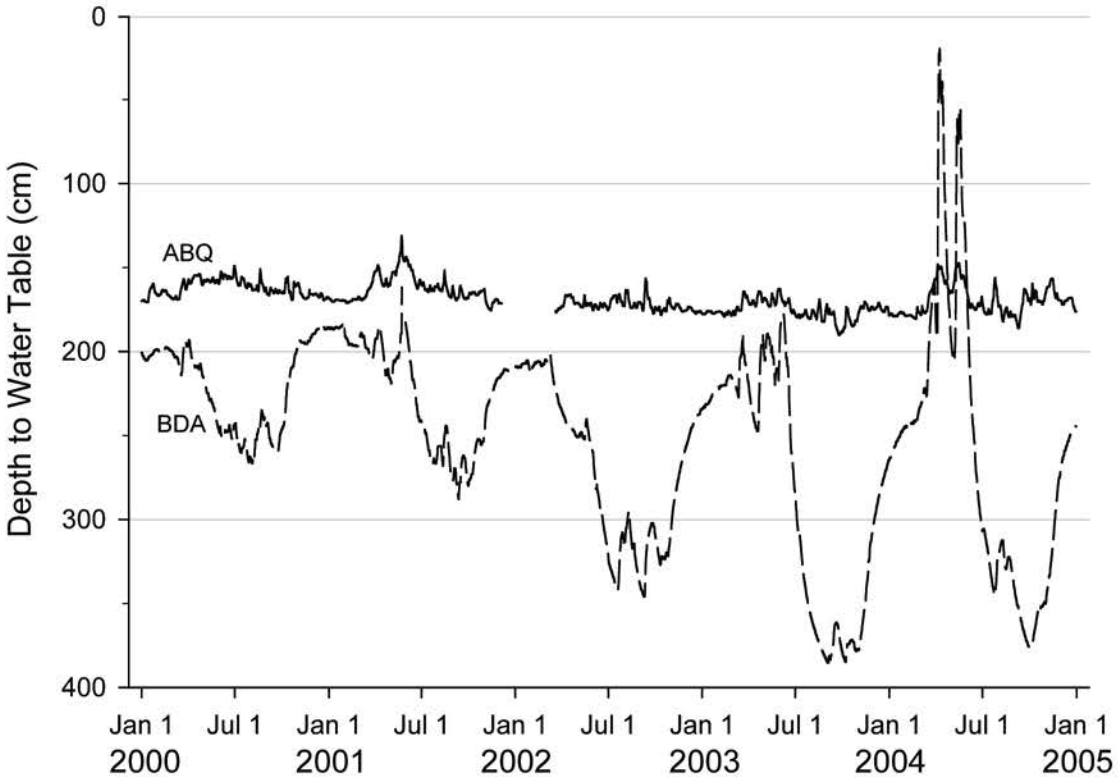
Depth to Water Table (cm)
0
100
200
300
400
ABQ
BDA
Jan 1
2000
Jul 1
Jan 1
2001
Jul 1
Jan 1
2002
Jul 1
Jan 1
2003
Jul 1
Jan 1
2004
Jul 1
Jan 1
2005

Figure 3:

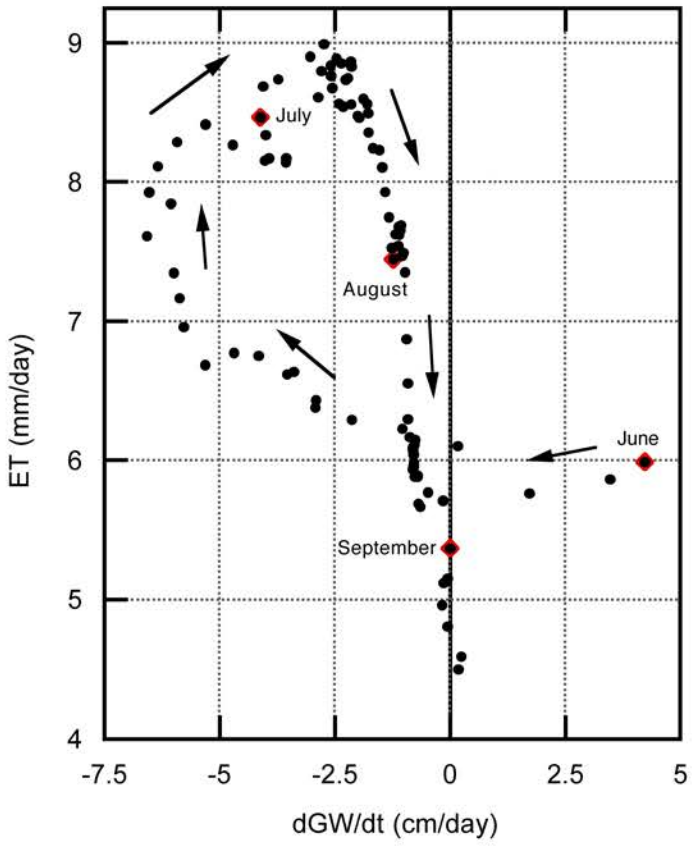
9
8
7
6
5
4
ET (mm/day)
July
August
June
September
-7.5
-5
-2.5
0
2.5
5
dGW/dt (cm/day)

Figure 4:

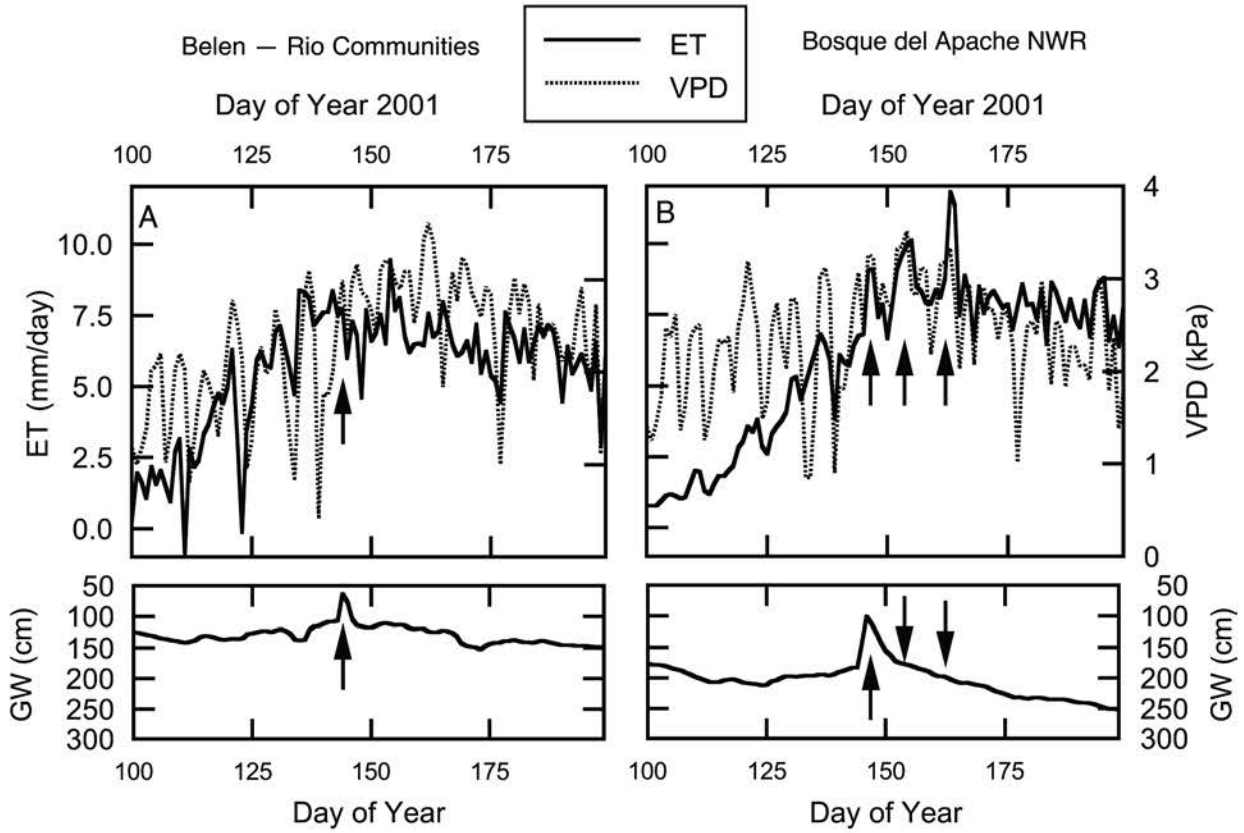
Belen — Rio Communities
ET
VPD
Bosque del Apache NWR
Day of Year 2001
Day of Year 2001
A
B
ET (mm/day)
VPD (kPa)
GW (cm)
GW (cm)
Day of Year
Day of Year

Figure 5:

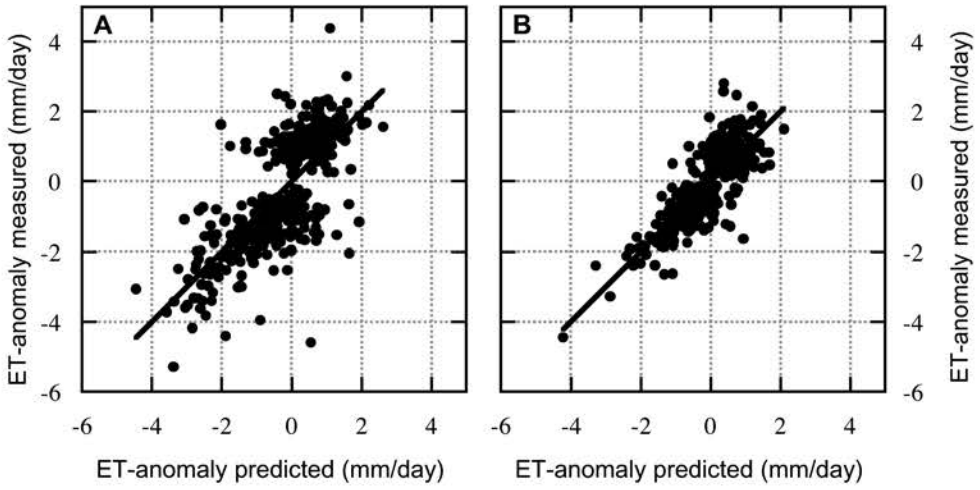
A
B
ET-anomaly measured (mm/day)
ET-anomaly predicted (mm/day)
ET-anomaly predicted (mm/day)
ET-anomaly measured (mm/day)
4
2
0
-2
-4
-6
-6
-4
-2
0
2
4